XLI CILAMCE
XLI Ibero-Latin American Congress on Computational Methods in Engineering
16-19 November, 2020 FOZ DO IGUAÇU PARANÁ - BRAZIL

Influence of circumferential discontinuity of an elastic foundation on the nonlinear dynamics of cylindrical shells with functionally graded material

Jonathas K. A. Pereira[1], Renata M. Soares[1], Frederico M. A. Silva[1]

[1] *School of Civil and Environmental Engineering, Federal University of Goiás, Avenida Universitária, 1488, Setor Leste Universitário, 74605-200, Goiânia, GO, Brasil*
jonathaskennedy@yahoo.com.br, renatasoares@ufg.br, silvafma@ufg.br

Abstract. In this paper we analyze the nonlinear vibrations of cylindrical shells, composed by functionally graded material, on an elastic foundation with circumferential discontinuity. The equilibrium equations are obtained from Donnell nonlinear theories and the elastic foundation is represented by Winkler model. The standard Galerkin's method was applied to discretize the differential partial equations and the perturbation method is used to describe the modal coupling of the solution that will be used in analysis. The nonlinear vibration of the shell will be studied through the frequency spectrum and frequency-amplitude relation, investigating the influence of some system parameters and the proposed modal solution for the transverse displacement field. Resonance curves for nonlinear forced vibrations and phase portrait are also evaluated, showing the complex behavior of nonlinear oscillations of shells with discontinuity of the elastic foundation.

Keywords: discontinuous elastic base, cylindrical shell, nonlinear dynamics, reduced order model.

1 Introduction

Cylindrical shells with discontinuity of the elastic base along its circumference can be found in various applications of these structures. However, few studies on nonlinear vibrations are found for this type of discontinuity of the elastic base and most studies focus on the analysis of problems with elastic foundation throughout its surface.

Amabili and Dalpiaz [1] investigated a linear analysis of cylindrical shells resting on elastic foundation with circumferential discontinuity. In their approach, the authors consider an expansion of the displacement field in Fourier series and the problem of eigenvalue is obtained through the Rayleigh quotient. Natural frequencies were obtained, and the results compared with a finite element model. In this issue, there are parametric studies developed by Tj et al. [2, 3] that demonstrated the behavior of linear vibrations of the cylindrical shell according to the distribution of the elastic foundation.

Nejad and Bideleh [4] studied the free nonlinear vibration of cylindrical shells on an elastic foundation subjected to a lateral loading, according to Sanders theory and considering the discontinuous elastic base on the circumferential direction of the shell. Sheng and Wang [5] presented an investigation of the dynamic behavior of elastic-based cylindrical shells across their surface, demonstrating, from a parametric analysis, that the phenomenon is quite complex resulting in a different nonlinear behaviors of the softening or hardening type.

Rodrigues [6] and Silva et al. [7] analyzed the nonlinear vibrations considering the discontinuity in the longitudinal direction of the cylindrical shell, demonstrating that depending on the position where there is no elastic base the forced vibrations of the system are much greater than the vibrations of a cylindrical shell totally in contact with an elastic base.

2 Mathematical formulation

Consider a cylindrical shell with radius R and thickness h, where $h << R$, length L and without initial geometric imperfections. Figure 1(a) shows the cylindrical shell's geometry as well as its displacement fields in axial (u), circumferential (v) and transversal (w) directions with its coordinate axes of the used system, namely: x, θ and z. The cylindrical shell is composed of a functional graded material, which varies in the direction of thickness, and is simply supported on a discontinuous elastic foundation, delimited at its extremes by θ_E and θ_D, as shown in Fig. 1(b), and continuous in the longitudinal direction. The driver force is a time dependent lateral pressure given by:

$$P(t) = P_L W_\theta \sin\left(\frac{m\pi x}{L}\right)\cos(\omega_1 t). \tag{1}$$

Where P_L is the pressure amplitude, W_θ is a function that determines the distribution of loading in the circumferential direction, m is the number of half-waves in the longitudinal direction, ω_1 is the frequency of excitation of the lateral pressure and t is the time.

Donnell's nonlinear theory, which describes the deformation fields, rotations, and curvature changes of the middle surface - in terms of displacements u, v and w - is given by:

$$\left[\varepsilon_{x0},\ \varepsilon_{\theta 0},\ \gamma_{x\theta 0}\right] = \left[u_{,x} + \frac{1}{2}w_{,x}{}^2,\ \frac{1}{R}\left(v_{,\theta} + w\right) + \frac{w_{,\theta}{}^2}{2R^2},\ \frac{1}{R}u_{,\theta} + v_{,x} + \frac{w_{,x}w_{,\theta}}{R}\right]; \tag{2}$$

$$\left[\beta_{x0},\ \beta_{\theta 0},\ \kappa_{x0},\ \kappa_{\theta 0},\ \kappa_{x\theta 0}\right] = \left[-w_{,x},\ -\frac{w_{,\theta}}{R},\ w_{,xx},\ -\frac{w_{,\theta\theta}}{R^2},\ -\frac{2w_{,x\theta}}{R}\right]. \tag{3}$$

Where eq. (2) relates to the deformation field while eq. (3) relates to the rotations and the curvature changes.

The elastic foundation is represented by a Winkler model with K_W stiffness modulus and the discontinuity of the elastic base is given by a Heaviside function, $H(\theta)$, where the origin of the axis of circumferential coordinates can be seen in Fig. 1(b). From this, the reaction equation of the elastic base is given by:

$$P_B = -K_W w\left[H\left(\theta - \theta_E\right) - H\left(\theta - \theta_D\right)\right]. \tag{4}$$

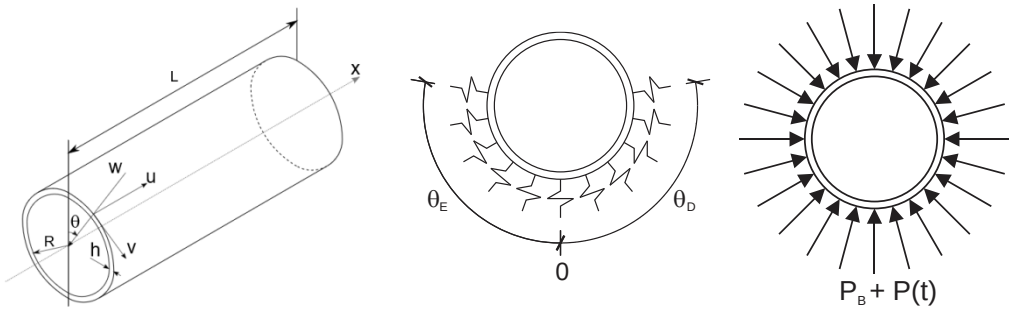

(a) (b) (c)

Figure 1. Shell characteristics (a) geometry (b) circumferential discontinuity and (c) harmonic lateral pressure

Equation (5) represents the nonlinear equilibrium equations of the cylindrical shell, described in terms of internal resultants where N_x, N_θ, $N_{x\theta}$ are membrane stresses and M_x, M_θ, $M_{x\theta}$ are bending and torsional moments, ∇^4 is the bi-harmonic operator of Laplace in cylindrical coordinates, η_1 is viscous damping, η_2 is the elastic viscous damping of the material, ω_0 is the natural frequency of cylindrical shell and ρ_1 is the average density of the material distributed in the thickness of the shell.

The resulting internal forces and moments are given in terms of deformations and changes in curvatures of the middle surface and they are presented in eq. (6), where A_{ij}, B_{ij}, C_{ij} (i,j = 1, 2, 6) are the terms of the elastic constitutive matrix that consider the effect of graded material. The physical parameters, E, ρ and v are described assuming a sandwich distribution, ranging as $P = (P_A - P_C)V_A(z) + P_C$, where P_A and P_C are the properties of

materials A and C, respectively, and $V_A(z) = (1-4z^2/h^2)^{2N+1}$ is the sandwich gradation equation [6, 7].

$$
\begin{aligned}
&-N_{x,x} - \frac{1}{R} N_{x\theta,\theta} = 0, \; -\frac{1}{R} N_{\theta,\theta} - N_{x\theta,x} = 0, \\
&\rho_1 \ddot{w} - M_{x,xx} - \frac{2}{R} M_{x\theta,x\theta} - \frac{1}{R^2} M_{\theta\theta,\theta\theta} + \frac{N_\theta}{R} + \left(N_x \beta_{x0} + N_{x\theta} \beta_{\theta 0}\right)_{,x} + \frac{1}{R}\left(N_{x\theta} \beta_{x0} + N_\theta \beta_{\theta 0}\right)_{,\theta} \\
&-P_B - P_L = -2\eta_1 \rho_1 \omega_0 \dot{w} - \eta_2 C_{11} \nabla^4 \dot{w}.
\end{aligned}
\tag{5}
$$

$$
\begin{Bmatrix} N_x \\ N_\theta \\ N_{x\theta} \\ M_x \\ M_\theta \\ M_{x\theta} \end{Bmatrix} = \begin{bmatrix} A_{11} & A_{12} & 0 & B_{11} & B_{12} & 0 \\ A_{12} & A_{11} & 0 & B_{12} & B_{11} & 0 \\ 0 & 0 & A_{66} & 0 & 0 & B_{66} \\ B_{11} & B_{12} & 0 & C_{11} & C_{12} & 0 \\ B_{12} & B_{11} & 0 & C_{12} & C_{11} & 0 \\ 0 & 0 & B_{66} & 0 & 0 & C_{66} \end{bmatrix} \begin{Bmatrix} \varepsilon_{x0} \\ \varepsilon_{\theta 0} \\ \varepsilon_{x\theta 0} \\ \kappa_{x0} \\ \kappa_{\theta 0} \\ \kappa_{x\theta 0} \end{Bmatrix}, \quad \left(A_{ij}, B_{ij}, C_{ij}\right) = \int_{-h/2}^{+h/2} Q_{ij}\left(1, z, z^2\right) dz \quad . \tag{6}
$$

$$
Q_{11} = \frac{E}{1-\nu^2}, \; Q_{12} = \frac{E\nu}{1-\nu^2}, \; Q_{66} = \frac{E}{2(1-\nu)}
$$

2.1 Reduced-order model in the circumferential direction of the shell

Consider a simply supported perfect cylindrical shell with radius R=0.6 m, length L=0.6 m, thickness h=0.003 m and θ_D=-θ_E=22.5º. The materials of functional gradation are: steel, called material A, and a ceramic material, called material C. The properties of the materials are: E_A= 205.1 × 10^9 N/m^2, ρ_A= 8900 kg/m^3, ν_A= 0.31, E_C= 322.3 × 10^9 N/m^2, ρ_C= 2370 kg/m^3 and ν_C= 0.24. In the analyses that will be presented the stiffness modulus of the elastic base is dimensioned according to $K_W = K_{nW} A_{11}/R^2$.

According to Silva et al. [8], in the cylindrical shells the natural frequencies occur in pairs with where the vibration modes are described by cos($n\theta$) or sin($n\theta$) in the circumferential direction. Here, n is the number of circumferential waves. However, for problems with circumferential discontinuity in the elastic foundation, the vibration modes and the natural frequencies are different with the transversal displacement field written as a Fourier series [1].

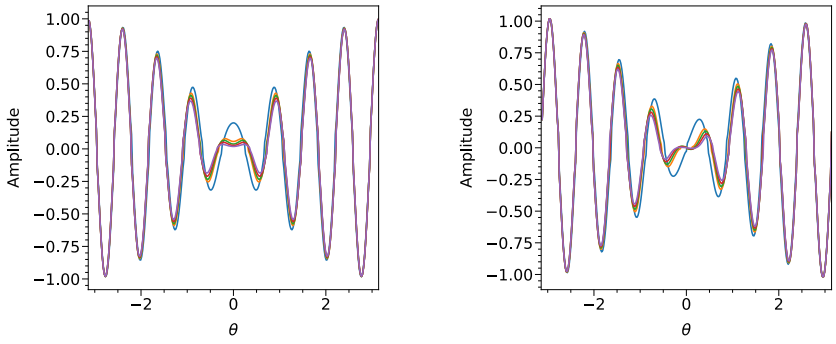

Figure 2. Vibration mode of a cylindrical shell for different K_{nW} values. (a) “Cosine mode” and (b) “Sine mode”. — K_{nW} = 0.003, — K_{nW} = 0.015, — K_{nW} = 0.03, — K_{nW} = 0.06 and — K_{nW} = 0.12.

Figure 2 shows the amplitude of vibration modes for x=L/2 for different stiffness of elastic bases that were obtained using ABAQUS® FEM software, using a mesh with S4R elements that guarantees the convergence to obtain the natural frequencies of the cylindrical shell with discontinuous elastic base. We use ABAQUS® FEM software as a strategy to investigate the main terms of a given Fourier series that participate in the natural vibration mode of the cylindrical shell resting on a discontinuous elastic base. The "Cosine modes" and "Sine modes" are thus named because they refer to the Fourier series that generates these vibration modes due to the uncoupled problem [1]. To obtain a reduced order model to describe the vibration mode of the problem appropriately, the Fourier transform is applied to the results obtained from finite element software. For the quantification of the participation of each modal expansion, the Parseval theorem is considered, eq. (7),

assuming that the velocity has a law analogous to the transversal displacement.

$$\int_L \int_h \int_{2\pi R} \rho \dot{f}(\theta)^2 \, d\theta \, dz \, dx = \frac{\omega_0^2}{2\pi} \int_L \int_h \int_\omega \rho F(\mathrm{i}\omega)^2 \, d\omega \, dz \, dx \tag{7}$$

In eq. (7), ω_0 is the natural frequency of the shell and F(iω) is the amplitude of the frequency obtained by the Fourier transform. Also, in eq. (7) it is possible to relate the participation of frequencies, which generate each mode of vibration, in kinetic energy. The region of most relevant frequencies will be the one that directly has the greatest contribution in the kinetic energy of the cylindrical shell. Then, the methodology for determining these regions is based on the percentage contribution of the sum of the squares of the amplitudes in the region of frequencies delimited to an acceptance criterion.

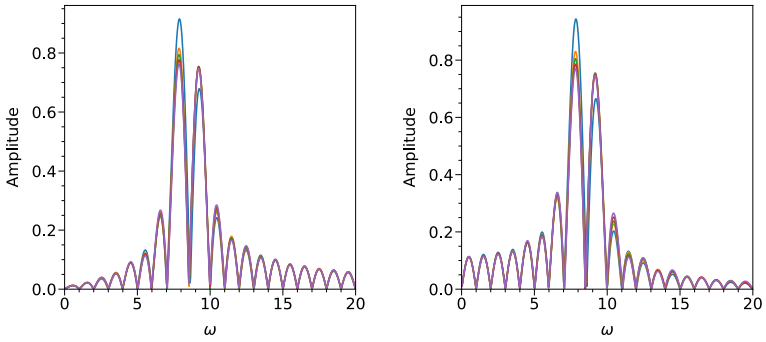

Figure 3. Frequency spectrum of a cylindrical shell for different K_{nW} values. (a) “Cosine mode” and (b) “Sine mode”. — K_{nW} = 0.003, — K_{nW} = 0.015, — K_{nW} = 0.03, — K_{nW} = 0.06 and — K_{nW} = 0.12

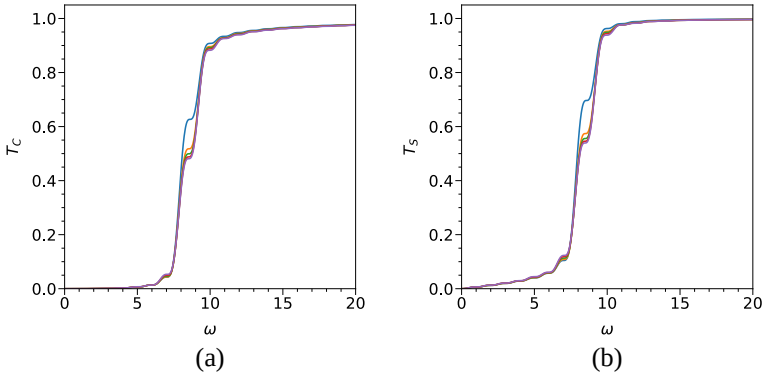

Figure 4. Accumulated energy in frequency domain for different K_{nW} values. (a) “Cosine mode” and (b) “Sine mode”. — K_{nW} = 0.003, — K_{nW} = 0.015, — K_{nW} = 0.03, — K_{nW} = 0.06 and — K_{nW} = 0.12

Figure 3 shows the frequency spectrum of the models and Fig. 4 shows the accumulated sum of eq. (7), where it is observed that in the region $7 \leq \omega \leq 9$ represents 80% and 85% total kinetic energy when analyzed, respectively, the "Cosine modes" and "Sine modes". Then, to obtain the nonlinear modal solution of this model associated with the main vibration modes the following initial solution will be adopted in the perturbation method to obtain a reduced order model to displacement field [6-10]:

$$w_0^C = \bar{W}_{8,1}^C(\tau)\cos(8\theta)\sin(q\xi) + \bar{W}_{9,1}^C(\tau)\cos(9\theta)\sin(q\xi); \tag{8}$$

$$w_0^S = \bar{W}_{8,1}^S(\tau)\sin(8\theta)\sin(q\xi) + \bar{W}_{9,1}^S(\tau)\sin(9\theta)\sin(q\xi). \tag{9}$$

Being, in eq. (8) and eq.(9), $q = m\pi$, $\xi = x/L$, with $0 \leq \xi \leq 1$ and $m = 1$. The modal solution was derived through the perturbation method - using as seed solution eq. (8) or eq.(9) - is presented containing all the degrees of freedom that arise from the modal couplings of the quadratic and cubic terms that are present in the equation

of nonlinear equilibrium of the cylindrical shell:

$$\begin{aligned}\left\{w^C,\, w^S\right\} = {} & W^X_{8,1}+W^X_{9,1}+W^X_{0,0}+W^X_{1,0}+W^X_{16,0}+W^X_{17,0}+W^X_{18,0}+W^X_{7,1}+W^X_{10,1}+W^X_{24,1}+W^X_{25,1}+W^X_{26,1}+\\ & W^X_{27,1}+W^X_{7,3}+W^X_{8,3}+W^X_{9,3}+W^X_{10,3}+W^X_{24,3}+W^X_{25,3}+W^X_{26,3}+W^X_{27,3}.\end{aligned} \tag{10}$$

Where in eq. (10) the following simplification was adopted, being $\tau = t\omega_0$:

$$\begin{aligned}&\left\{W^C_{i,\beta}, W^S_{i,\beta}\right\} = \left\{\bar{W}^C_{i,\beta}(\tau)\cos(i\theta), \bar{W}^S_{i,\beta}(\tau)\sin(i\theta)\right\}\sin(\beta q\xi) \qquad \text{to } \beta = \{1,3\},\\ &\left\{W^C_{i,0}, W^S_{i,0}\right\} = \left\{\bar{W}^C_{i,0}(\tau), \bar{W}^S_{i,0}(\tau)\right\}\cos(i\theta)\left[\frac{3}{4}-\cos(2q\xi)+\frac{1}{4}\cos(4q\xi)\right].\end{aligned} \tag{11}$$

The modal solution for the displacements field, *u* and *v*, with their modal couplings are obtained by expanding these displacements in terms of modal solution *w*. Applying the procedure proposed by Silva [9] and Gonçalves et al. [10] a consistent system is obtained for the displacement fields *u* and *v*, given by:

$$\begin{aligned}\left\{u^C,\, u^S\right\} = {} & U^X_{8,1}+U^X_{9,1}+U^X_{8,3}+U^X_{9,3}+U^X_{8,5}+U^X_{9,5}+U^X_{8,7}+U^X_{9,7}+U^X_{0,2}+U^X_{1,2}+U^X_{16,2}+U^X_{17,2}+\\ & U^X_{18,2}+U^X_{0,6}+U^X_{1,6}+U^X_{16,6}+U^X_{17,6}+U^X_{18,6}+U^X_{7,1}+U^X_{10,1}+U^X_{24,1}+U^X_{25,1}+U^X_{26,1}+\\ & U^X_{27,1}+U^X_{7,3}+U^X_{10,3}+U^X_{24,3}+U^X_{25,3}+U^X_{26,3}+U^X_{27,3}+U^X_{7,5}+U^X_{10,5}+U^X_{24,5}+U^X_{25,5}+\\ & U^X_{26,5}+U^X_{27,5}+U^X_{7,7}+U^X_{10,7}+U^X_{24,7}+U^X_{25,7}+U^X_{26,7}+U^X_{27,7}+U^X_{2,2}+U^X_{15,2}+U^X_{19,2}+U^X_{32,2}+\\ & U^X_{33,2}+U^X_{34,2}+U^X_{35,2}+U^X_{36,2}+U^X_{2,6}+U^X_{15,6}+U^X_{19,6}+U^X_{32,6}+U^X_{33,6}+U^X_{34,6}+U^X_{35,6}+U^X_{36,6};\end{aligned} \tag{12}$$

$$\begin{aligned}\left\{v^C,\, v^S\right\} = {} & V^X_{8,1}+V^X_{9,1}+V^X_{8,3}+V^X_{9,3}+V^X_{8,5}+V^X_{9,5}+V^X_{8,7}+V^X_{9,7}+V^X_{1,0}+V^X_{16,0}+V^X_{17,0}+V^X_{18,0}+V^X_{1,4}+\\ & V^X_{16,4}+V^X_{17,4}+V^X_{18,4}+V^X_{7,1}+V^X_{10,1}+V^X_{24,1}+V^X_{25,1}+V^X_{26,1}+V^X_{27,1}+V^X_{7,3}+V^X_{10,3}+V^X_{24,3}+\\ & V^X_{25,3}+V^X_{26,3}+V^X_{27,3}+V^X_{7,5}+V^X_{10,5}+V^X_{24,5}+V^X_{25,5}+V^X_{26,5}+V^X_{27,5}+V^X_{7,7}+V^X_{10,7}+V^X_{24,7}+\\ & V^X_{25,7}+V^X_{26,7}+V^X_{27,7}+V^X_{2,0}+V^X_{15,0}+V^X_{19,0}+V^X_{32,0}+V^X_{33,0}+V^X_{34,0}+V^X_{35,0}+V^X_{36,0}+V^X_{2,4}+\\ & V^X_{15,4}+V^X_{19,4}+V^X_{32,4}+V^X_{33,4}+V^X_{34,4}+V^X_{35,4}+V^X_{36,4}.\end{aligned} \tag{13}$$

Where in eqs. (12) and (13) the following simplification was adopted, being $\tau = t\omega_0$:

$$\begin{aligned}&\left\{U^C_{i,\beta}, U^S_{i,\beta}\right\} = \left\{\bar{U}^C_{i,\beta}(\tau)\cos(i\theta), \bar{U}^S_{i,\beta}(\tau)\sin(i\theta)\right\}\cos(\beta q\xi) \qquad \text{to } \beta = \{1,3,5,7\},\\ &U^X_{i,\beta} = \bar{U}^X_{i,\beta}(\tau)\cos(i\theta)\left[sen(\beta q\xi)-\frac{\beta}{\beta+2}sen\left((\beta+2)q\xi\right)\right] \qquad \text{to } \beta = \{2,6\},\\ &\left\{V^C_{i,\beta}, V^S_{i,\beta}\right\} = \left\{\bar{V}^C_{i,\beta}(\tau)\cos(i\theta), \bar{V}^S_{i,\beta}(\tau)\sin(i\theta)\right\}\sin(jq\xi) \qquad \text{to } \beta = \{1,3,5,7\},\\ &V^X_{i,\beta} = \bar{V}^X_{i,\beta}(\tau)\sin(i\theta)\left[\cos(\beta q\xi)-\cos\left((\beta+2)q\xi\right)\right] \qquad \text{to } \beta = \{0,4\}.\end{aligned} \tag{14}$$

From the obtained modal solutions, the reduced order models are assembled in the following form: the model of "Cosine modes" consists of modal expansions (u^C, v^S, w^C) and "Sine modes" with (u^S, v^C, w^S). The Galerkin method is applied to discretize the partial differential equations of eq. (5), obtaining a nonlinear system of second-order equations in relation to τ where the amplitudes of *u* and *v* can be written in terms of *w*.

3 Numerical results and discussions

In numerical results that will be presented below, the physical and geometric parameters was defined in the previous section and a non-dimensional value of the elastic base is given by $K_{nW} = 0.003$. In analysis of resonance curves, consider the viscous damping $\eta_1 = 0.001$, the elastic viscous damping $\eta_2 = 0$, the amplitude of lateral harmonic pressure $P_L = 5000$ N/m² and $W_\theta = [P_{8C}\cos(8\theta) + P_{8S}\sin(8\theta) + P_{9C}\cos(9\theta) + P_{9S}\sin(9\theta)]\sin(q\xi)$ where the terms: P_{8C}, P_{8S}, P_{9C} and P_{9C} are a 0-1 factor that excites directly the modes that are in the initial solution of the perturbation method.

Figure 5 shows the nonlinear frequency-amplitude relation for the "Cosine modes" and "Sine modes" which they were obtained using the shooting method [8]. The convergence analysis is carried out by adding the terms of greater order of the expansion *w*. It is observed that only with the inclusion of the terms of the third order of *w*, which are those generated by the modal coupling derived from the cubic terms, are sufficient for a

convergence up to the amplitude of the shell thickness for both "Cosine modes" and "Sine mode" models.

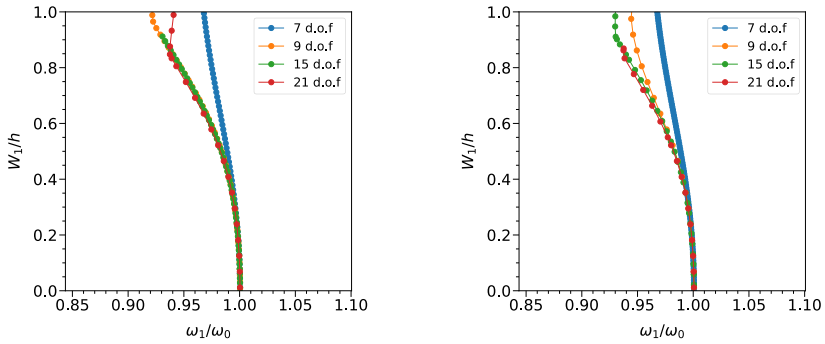

Figure 5. Convergence of the frequency-amplitude relation for both: (a) “cosine mode” and (b) “sine mode”, considering a simply supported cylindrical shell. 7-dof: $W_{8,1} + W_{9,1} + W_{0,0} + W_{1,0} + W_{16,0} + W_{17,0} + W_{18,0}$. 9-dof: $W_{8,1} + W_{9,1} + W_{0,0} + W_{1,0} + W_{16,0} + W_{17,0} + W_{18,0} + W_{8,3} + W_{9,3}$. 15-dof: $W_{8,1} + W_{9,1} + W_{0,0} + W_{1,0} + W_{16,0} + W_{17,0} + W_{18,0} + W_{8,3} + W_{9,3} + W_{7,1} + W_{10,1} + W_{24,1} + W_{25,1} + W_{26,1} + W_{27,1}$. 21-dof: $W_{8,1} + W_{9,1} + W_{0,0} + W_{1,0} + W_{16,0} + W_{17,0} + W_{18,0} + W_{8,3} + W_{9,3} + W_{7,1} + W_{10,1} + W_{24,1} + W_{25,1} + W_{26,1} + W_{27,1} + W_{7,3} + W_{10,3} + W_{24,3} + W_{25,3} + W_{26,3} + W_{27,3}$.

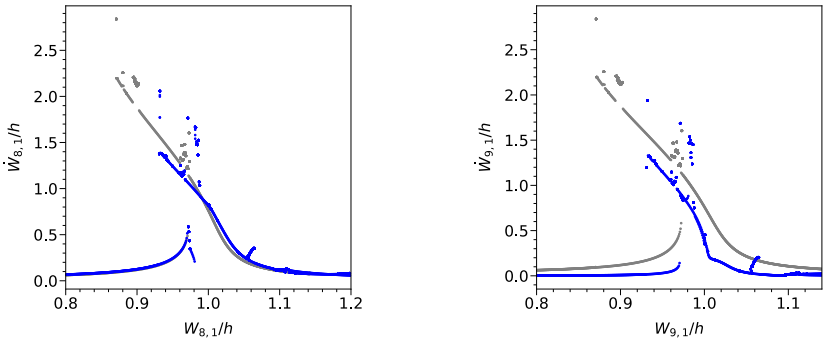

Figure 6. Resonance curves for a simply supported cylindrical shell and “Cosine mode”. The gray curve represents a cylindrical shell resting on elastic base without discontinuity while the blue curve represents the cylindrical shell resting on discontinuous elastic base (a) $W_{8,1}$, (b) $W_{9,1}$. (K_{nW} = 0.003, P_{8C} = 1, P_{8S}=P_{9C}=P_{9S} = 0)

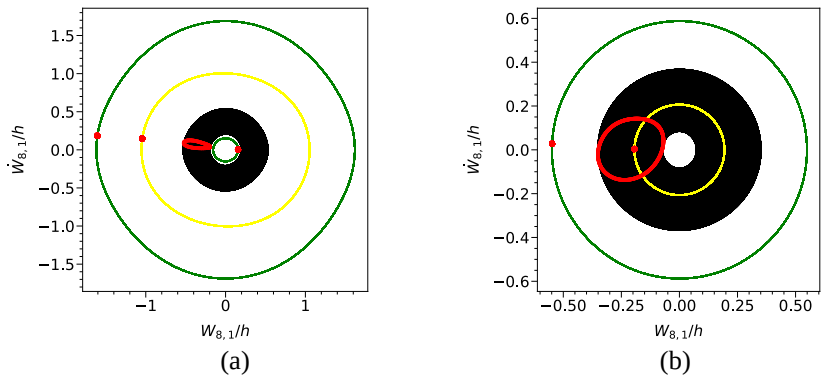

Figure 7. Phase-portrait with Poincaré map for “Cosine mode” for a simply supported cylindrical shell: (a) ω_1/ω_0 = 0.972, (b) ω_1/ω_0 = 1.064. (K_{nW} = 0.003, P_{8C} = 1, P_{8S}=P_{9C}=P_{9S} = 0)

Figure 6 shows the resonance curves obtained for the excitation mode (m = 1, n = 8 , P_{8C} = 1, P_{8S} = P_{9C} = P_{9S} = 0) of the harmonic pressure, considering the "Cosine mode" model. The gray resonances curves are related to a simply supported cylindrical surrounding by the same elastic base. From these resonance curves it is possible to

observe a complex behavior of the cylindrical shell with several dynamic jumps with a competition between resonant and non-resonant responses in the region close to the resonance. When its resonance curve is compared to a case surrounded by the elastic base, it is observed several changes in these results, indicating that the discontinuity on the elastic base can changes significantly the nonlinear response. The results also demonstrate that, for this case studied, the behavior of the cylindrical shell is quite similar between the fundamental modes of the shell, as can be seen for the amplitude $W_{8,1}$ - Fig. 6 (a) - and $W_{9,1}$ - Fig. 6 (b) - which they suggest an analysis of possible internal resonances between the fundamental modes. Due to discontinuity of the elastic base, it is still possible to observe the occurrence of both quasi-periodic (black phase portrait) and periodic (yellow phase portrait) responses along the resonance curves as shown in Fig 7 that did not occur for the surrounded case (green phase portrait).

4 Conclusions

In this paper, the nonlinear vibration of the shell with a circumferential discontinuity was studied through the frequency-response curve and frequency-amplitude relation, a low dimensional model was derived and an investigation of the influence of some system parameters and the proposed modal solution was evaluated. Resonance curves for nonlinear forced vibrations showed the complex behavior of nonlinear oscillations of shells with discontinuity of the elastic foundation and the importance of the modal coupling to obtain the reduced order model.

Acknowledgements. This work was supported by Brazilian Ministry of Education – CAPES.

Authorship statement. The authors hereby confirm that they are the sole liable persons responsible for the authorship of this work, and that all material that has been herein included as part of the present paper is either the property (and authorship) of the authors, or has the permission of the owners to be included here.

References

[1] Amabili, M.; Dalpiaz, G. (1997) Free Vibrations of Cylindrical Shells with Non-Axisymmetric Mass Distribution on Elastic Bed. Meccanica, 32, 71–84.
[2] Tj, H. G.; Mikami, T.; Kanie, S.; Sato, M. Free vibrations of fluid-filled cylindrical shells on elastic foundations. Thin-Walled Structures, v. 43, n. 11, p. 1746–1762, 2005.
[3] Tj, H. G.; Mikami, T.; Kanie, S.; Sato, M. Free vibration characteristics of cylindrical shells partially buried in elastic foundations. Journal of Sound and Vibration, v. 290, n. 3–5, p. 785–793, 2006.
[4] Nejad, F. B.; Bideleh, S. M. M. Nonlinear free vibration analysis of prestressed circularcylindrical shells on the Winkler/Pasternak foundation. Thin-Walled Structures, v. 53, p.26–39, 2012.
[5] Sheng, G. G.; Wang, X.; Fu, G.; Hu, H. (2014) The Nonlinear Vibrations of Functionally Graded Cylindrical Shells Surrounded by an Elastic Foundation. Nonlinear Dyn, 78 , 1421–1434.
[6] Rodrigues, P. C. Influência da descontinuidade da base elástica nas curvas de ressonância de uma casca cilíndrica, 2019. Goiânia: Universidade Federal de Goiás.
[7] Silva, F. M. A.; Rodrigues, P. C.; Gonçalves, P. B. Nonlinear Oscillation of a FG Cylindrical Shell on a Discontinuous Elastic Foundation. In New Trends in Nonlinear Dynamics - Proceedings of the First International Nonlinear Dynamics Conference (NODYCON 2019); Lacarbonara, W., Balachandran, B., Ma, J., Machado, J. A. T., Stepan, G., Series Eds.; Springer: Roma, 2020; Vol. 3, pp 79–88.
[8] SILVA, F. M. A.; GONÇALVES, P. B.; DEL PRADO, Z. J. G. N. An alternative procedure for the non-linear vibration analysis of fluid-filled cylindrical shells. Nonlinear Dynamics, v. 66, n. 3, p. 303–333, 2011.
[9] SILVA, F. M. A. Modelos de dimensão reduzida para análise das oscilações não-lineares e estabilidade de cascas cilíndricas, 24. mar. 2008. Rio de Janeiro, Brazil: Pontifícia Universidade Católica do Rio de Janeiro.
[10] GONÇALVES, P. B.; SILVA, F. M. A.; DEL PRADO, Z. J. G. N. Low-dimensional models for the nonlinear vibration analysis of cylindrical shells based on a perturbation procedure and proper orthogonal decomposition. Journal of Sound and Vibration, v. 315, n. 3, p. 641–663, 2008.